Aquistore project: ground deformation retrieved by InSAR during May 2012 - May 2013

Sergey Samsonov
Canada Centre for Remote Sensing
Natural Resources Canada
588 Booth Street, Ottawa
ON K1A0Y7, Canada
sergey.samsonov@nrcan-rncan.gc.ca

Don White
Geological Survey of Canada
Natural Resources Canada
615 Booth Street
Ottawa, ON K1A0E9
don.white@nrcan-rncan.gc.ca

Michael Craymer
Geodetic Survey Division
Natural Resources Canada
615 Booth Street
Ottawa, ON K1A0E9
michael.craymer@nrcan-rncan.gc.ca

***Abstract*—Objectives of the Aquistore CO2 storage project are to design, adapt, and test non-seismic monitoring methods that have not been systematically utilized to date for monitoring CO2 storage, and to integrate the data from these various monitoring tools to obtain quantitative estimates of the change in subsurface fluid distributions, pressure changes and associated surface deformation. Since spring of 2012 RADARSAT-2 data from five beams (ascending and descending Spotlight, Wide UltraFine and Fine Quad-Pol) were regularly (with the individual frequency of 24 days) collected and used for calculation of ground deformation time series over the Aquistore CO2 storage site located in SE Saskatchewan. The initial InSAR analysis revealed slow ground deformation not related to CO2 injection but caused by various natural and anthropogenic processes - snow melt, surface moisture variation, ground and surface water level changes and post-mining activities. In this work we provide updated results based on over one hundred RADARSAT-2 images acquired during May 2012 - May 2013.**

I. Introduction

In this work we used Interferometric Synthetic Aperture Radar (InSAR) [1], [2] to map ground deformation over the Aquistore carbon sequestration site located near the city of Estevan in Saskatchewan, Canada (Fig 1). InSAR methodology has been used in the past for monitoring ground deformation of natural [3]–[5] and anthropogenic [6], [7] origins. In favorable conditions with InSAR it is possible to achieve sub-centimeter precision measuring deformation rates and to detect transient signals if temporally dense data sets are available.

InSAR measurements are usually affected by various noise sources (orbital, atmospheric, topographic, etc.) that can be mitigated by performing an advanced analysis [8]–[11]. In the Saskatchewan region InSAR is also susceptible to seasonal noise due to snow coverage, soil freezing, seasonal changes in vegetation, and to the anthropogenic noise due to settlement of post-mining landfill. The RADARSAT-2 data (Table I) from five beams was acquired on average every five days during May 2012 - May 2013 period. Advanced InSAR analysis based on the Multidimensional Small Baseline (MSBAS) method [12] was performed that produced a vertical deformation rate map and a time series of ground deformation.

II. Results

The vertical deformation rate map is shown in Fig 3 and time series of vertical deformation for selected points are

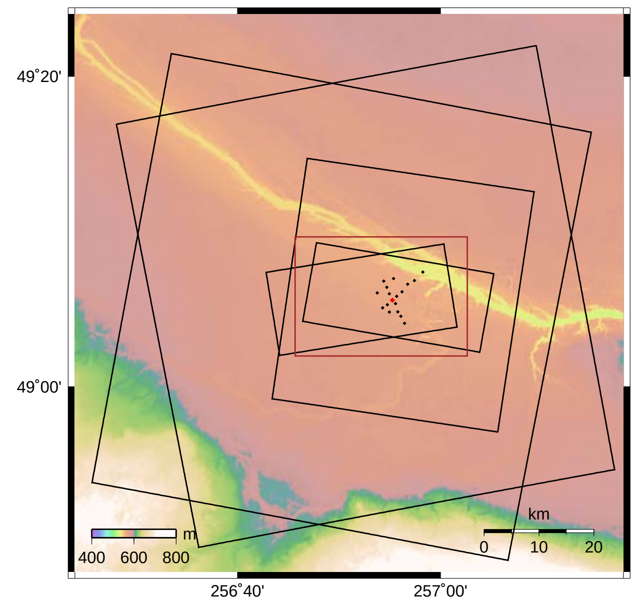

Fig. 1. Area of interest is outlined in brown, RADARSAT-2 frames used in this study are outlined in black: large frames are from ascending and descending Wide Ultra-Fine (U7W2), smallest frames are from ascending Spotlight (SLA18) and descending Spotlight (SLA12) and remaining frame is from descending Fine Quad-Pol (FQ28) beams. Digital Elevation Model is plotted in background. Black diamonds mark locations of observation sites and red diamond marks location of injection well.

shown in Fig 2. Injection well is located at the SITE location and additional instrumentation sites are marked with NE, NW, SE, and SW labels corresponding to their approximate direction. The observed deformation rate at these sites does not exceed ± 1 cm/year. The observed signal is most likely due to seasonal changes and snow coverage contaminated by the measurement noise smoothed by filtering during MSBAS processing.

We also observe areas with relatively fast (>1 cm/year) motion. These uplift regions are marked as points U1-U5 and subsidence is marked as S1. The cause of this deformation is presently unknown and will be investigated in the future.

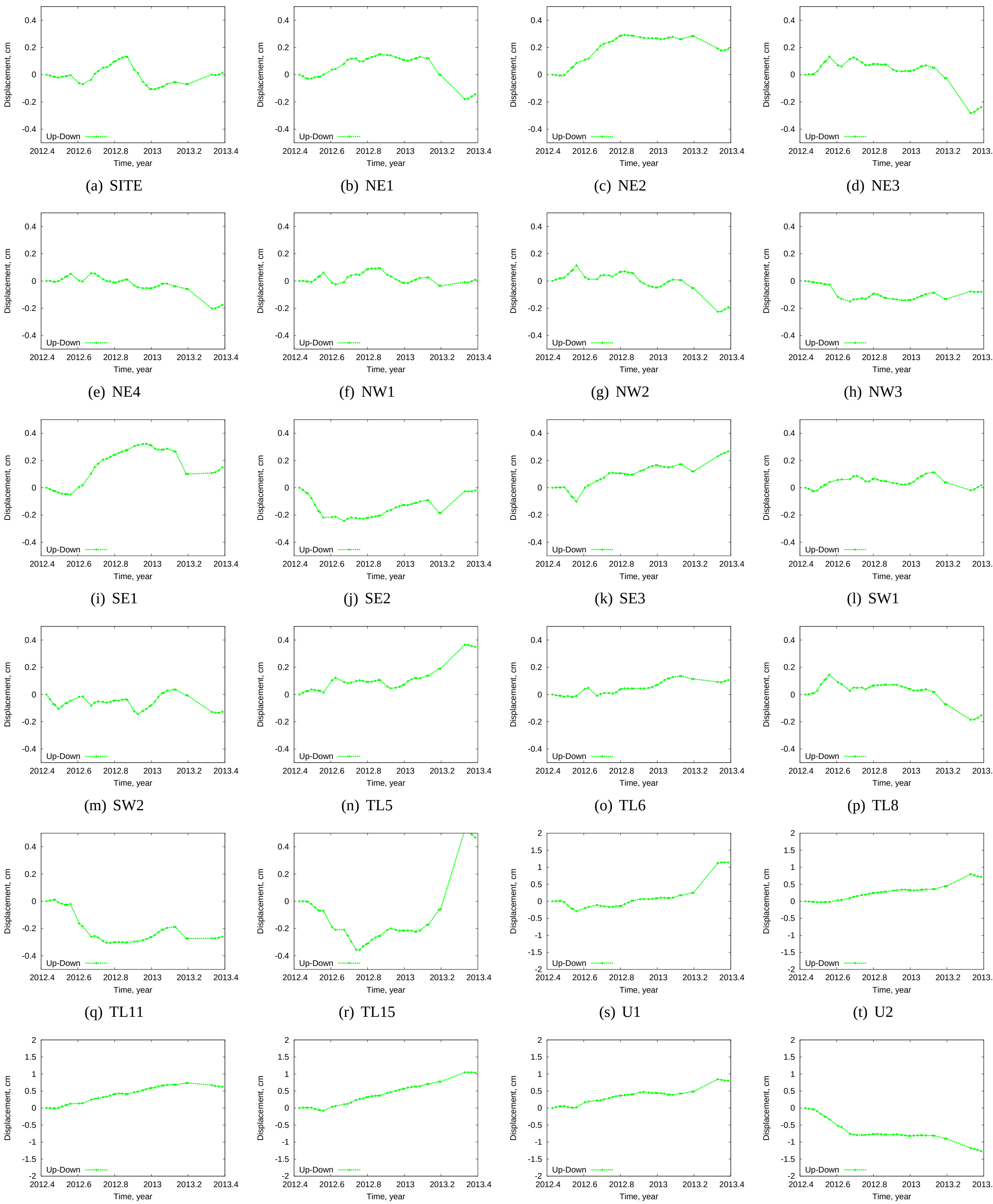

(a) SITE (b) NE1 (c) NE2 (d) NE3
(e) NE4 (f) NW1 (g) NW2 (h) NW3
(i) SE1 (j) SE2 (k) SE3 (l) SW1
(m) SW2 (n) TL5 (o) TL6 (p) TL8
(q) TL11 (r) TL15 (s) U1 (t) U2
(u) U3 (v) U4 (w) U6 (x) S1

Fig. 2. Time series of vertical deformation. Points NE, NW, SE and SW correspond to approximate locations of observation sites and point SITE corresponds to location of injection well. Points U1-U5 experience faster than normal uplift and point S1 experiences faster than normal subsidence. Note change in scale for U1-U5 and S1 points.

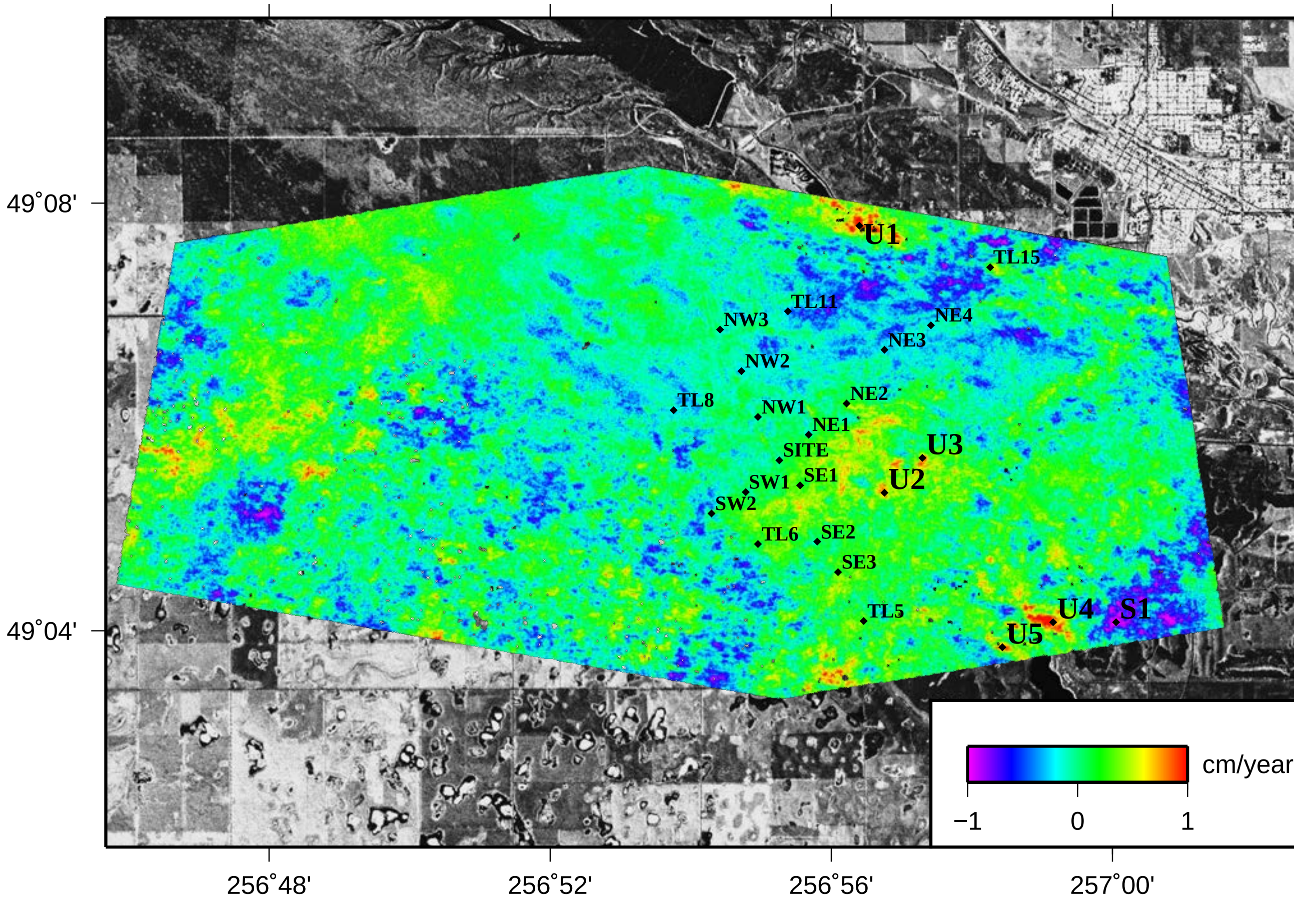

Fig. 3. Vertical linear deformation rate calculated from five RADARSAT-2 beams with MSBAS method [12], [13]. Locations of observation sites (NE, NW, SE and SW) and injection well (SITE) are marked with black diamonds. In background is SAR intensity image. For points U1-U5 and S1 ground deformation rate exceeds background values.

TABLE I. SAR DATA SETS USED IN THIS STUDY: TIME SPAN (IN YYYYMMDD FORMAT), RANGE-AZIMUTH RESOLUTION, RANGE-AZIMUTH COVERAGE, AZIMUTH θ AND INCIDENCE ϕ ANGLES, AND NUMBER OF AVAILABLE SAR IMAGES N FOR EACH DATA SET.

InSAR set	Time span	Res., m	Cov., km	θ°	ϕ°	N
U7W2 asc	20120619-20130521	1.6-2.8	50-50	349	35	11
U7W2 dsc	20120615-20130423	1.6-2.8	50-50	-170	35	11
SLA18 asc	20120605-20130531	1.6-0.8	18-8	351	43	14
SLA11 dsc	20120622-20130524	1.6-0.8	18-8	-170	39	14
FQ28 dsc	20120612-20130514	5.2-7.6	25-25	-172	47	14

III. CONCLUSIONS

The vertical deformation rate map with corresponding time series presented here demonstrate background noise. These signals need to be properly understood and, if possible, corrected to increase the measuring precision necessary to detect the slow deformation that may be produced by CO2 injection.

ACKNOWLEDGEMENT

We thank the Canadian Space Agency (CSA) for providing RADARSAT-2 data. Figures were plotted with GMT and gnuplot software.

REFERENCES

[1] D. Massonnet and K. Feigl, “Radar interferometry and its application to changes in the Earth surface,” *Reviews of Geophysics*, vol. 36, no. 4, pp. 441–500, 1998.

[2] P. Rosen, P. Hensley, I. Joughin, F. Li, S. Madsen, E. Rodriguez, and R. Goldstein, “Synthetic aperture radar interferometry,” *Proceedings of the IEEE*, vol. 88, no. 3, pp. 333–382, 2000.

[3] Y. Fialko, “Interseismic strain accumulation and the earthquake potential on the southern San Andreas fault system,” *Nature*, vol. 441, pp. 968–971, 2006.

[4] S. Samsonov, K. Tiampo, and J. Rundle, “Application of DInSAR-GPS optimization for derivation of three dimensional surface motion of southern California region along the San Andreas fault,” *Computers and Geosciences*, vol. 34, no. 5, pp. 503–514, 2008.

[5] R. Beavan, S. Samsonov, P. Denys, R. Sutherland, N. Palmer, and M. Denham, “Oblique slip on the Puysegur subduction interface in the 2009 July Mw 7.8 Dusky Sound earthquake from GPS and InSAR observations : implications for the tectonics of southwestern New Zealand.,” *Geophysical Journal International*, vol. 183, no. 3, pp. 1265–1286, 2010.

[6] S. Samsonov, K. Tiampo, P. Gonzalez, V. Manville, and G. Jolly, “Ground deformation occurring in the city of Auckland, New Zealand, and observed by Envisat interferometric synthetic aperture radar during 2003-2007,” *Journal of Geophysical Research - Solid Earth*, vol. 115, no. B08410, 2010.

[7] S. Samsonov, P. Gonzalez, K. Tiampo, and N. d’Oreye, “Methodology for spatio-temporal analysis of ground deformation occurring near Rice

Lake (Saskatchewan) observed by Radarsat-2 DInSAR during 2008-2011," *Canadian Journal of Remote Sensing*, vol. 39, no. 1, pp. 27–33, 2013.

[8] Z. Li, J.-P. Muller, P. Cross, and E. J. Fielding, "Interferometric synthetic aperture radar (InSAR) atmospheric correction: GPS, Moderate Resolution Imaging Spectroradiometer (MODIS), and InSAR integration," *Journal of Geophysical Research*, vol. 110, no. B03410, 2005.

[9] F. Meyer, R. Bamler, N. Jakowski, and T. Fritz, "The potential of low-frequency SAR systems for mapping ionospheric TEC distributions," *IEEE Geoscience and Remote Sensing Letters*, vol. 3, no. 4, pp. 560–564, 2006.

[10] S. Samsonov, "Topographic correction for ALOS PALSAR interferometry," *IEEE Transactions on Geoscience and Remote Sensing*, vol. 48, no. 7, pp. 3020 – 3027, 2010.

[11] S. Samsonov, M. van der Koij, and K. Tiampo, "A simultaneous inversion for deformation rates and topographic errors of DInSAR data utilizing linear least square inversion technique," *Computers and Geosciences*, vol. 37, no. 8, pp. 1083–1091, 2011.

[12] S. Samsonov and N. d'Oreye, "Multidimensional time series analysis of ground deformation from multiple InSAR data sets applied to Virunga Volcanic Province.," *Geophysical Journal International*, vol. 191, no. 3, pp. 1095–1108, 2012.

[13] S. Samsonov, N. d'Oreye, and B. Smets, "Ground deformation associated with post-mining activity at the French-German border revealed by novel InSAR time series method," *International Journal of Applied Earth Observation and Geoinformation*, vol. 23, pp. 142–154, 2013.